Supporting information.

How gold particles suppress concentration quenching of fluorophores encapsulated in silica beads.

Table I. Properties of different test samples studied. For a preparation of 1.75 mmol SiOx, are indicated the moles number of fluorescein used in the synthesis ($n_{FITCtotal}$), the moles number lost in the supernatant ($n_{FITClost}$), the efficiency of the fluorescein encapsulation, the number of fluorescein per volume unit of polysiloxane ($[FITC]_{SiOx}$), the inter-dye average distance within SiOx ($<d_{FITC}>$) and the number of fluorescein per particle ($\#_{FITC}$/particle).

Au core diameter (nm)	*Particle diameter (nm)*	*standard deviation (nm)*	$n_{FITCtotal}$ *(μmol)*	$n_{FITClost}$ *(μmol)*	*Efficiency (%)*	$[FITC]_{SiOx}$ *(mM)*	$<d_{FITC}>$ *(nm)*	$<\#_{FITC}/bead>$
0	63±3	9±1	6,93	2,32	67	219,7	2,0	14230
0	64±3	9±1	3,47	1,91	45	74,1	2,8	4798
0	63±3	9±1	1,73	1,19	32	26,0	4,0	1686
0	64±3	9±1	0,87	0,59	31	13,0	5,0	840
0	64±3	9±1	0,79	0,53	33	12,4	5,1	802
0	65±3	9±1	0,39	0,28	29	5,5	6,7	358
0	66±3	9±1	0,20	0,14	28	2,6	8,6	168
0	64±3	9±1	0,10	0,06	34	1,6	10,1	105
4.9±0.2	58±1	1.00±0.02	6,93	2,42	65	85,2	2,7	5517
4.9±0.2	58±1	1.00±0.02	3,47	1,47	58	37,6	3,5	2437
4.9±0.2	58±1	1.00±0.02	1,73	0,80	54	17,7	4,5	1145
4.9±0.2	58±1	1.00±0.02	0,87	0,39	54	8,9	5,7	577
4.8±0.2	58±1	1.00±0.02	0,79	0,40	49	7,3	6,1	476
4.9±0.2	58±1	1.00±0.02	0,39	0,19	51	3,8	7,6	247
4.9±0.2	58±1	1.00±0.02	0,20	0,09	53	2,0	9,5	127
4.8±0.2	58±1	1.00±0.02	0,10	0,04	59	1,1	11,5	71

1- Reasons for which a single population can be described by a multi-exponential law.

Concerning fluorescein in polysiloxane particles, the shape of the intensity decay does not follow the mono-exponential trend given by formula (6). This deviation from a mono-exponential behaviour was already observed for fluorescein embedded in silica particles in similar amounts. Two different arguments can explain this non-monoexponential trend.

First reason for which a single population can be described by a multi-exponential law.

First it can arise from the fact that (i) the lifetime depends on the concentration and (ii) the dye concentration within the particle is not homogeneous. Then a particle that presents fluctuations in concentration is not characterized by a unique lifetime but by a distribution in fluorescein lifetimes, each fluorescein molecule having a different local environment. Moreover, the intensity decay strongly increases with the quantity of dyes embedded indicating that lifetime decreases with concentration. This arises from the definition of τ ($\tau = \frac{1}{\Gamma_r + k_{nr}}$). Indeed, when $c \to 0$, the possibility of transfer from a monomer to a dimer that acts as trap for light is completely reduced and the contribution of self-quenching to the non-radiative decay rate completely vanishes so that k_{nr} is strongly decreased. Inversely when c increases, the probability of transfer to a quencher is greatly increased. k_{nr} is then increased and the lifetime decreased. Even if, in theory, each intensity decay curve should be fitted by a multi-exponential curve, it has been shown that a simpler fit of the experimental curve by a bi-exponential function is sufficient in many cases. In this paper, the curves have then been systematically fitted by the least-square method using the two-terms exponential function:

$$I(t) = \alpha_1 \exp\left(-t / \tau_1\right) + \alpha_2 \exp\left(-t / \tau_2\right)$$

In this latter equation α_1 and α_2 are amplitude coefficients and τ_1 and τ_2 ($\tau_1 > \tau_2$) the two decay times to determine. From an adequate combination of these phenomenological parameters, τ_1 (the slow lifetime) and τ_2 (the fast lifetime), an average lifetime $\bar{\tau}$ corresponding to an average dye concentration within the particle can be finally obtained:

$$\bar{\tau} = \frac{\alpha_1 \tau_1^2 + \alpha_2 \tau_2^2}{\alpha_1 \tau_1 + \alpha_2 \tau_2}$$

All the fit results are given in table II (supporting information) that details for each sample the values of τ_1, τ_2, α_1, α_2 and $\bar{\tau}$. For all concentrations except the lower, the ratio α_1 / α_2 is close to $50/50$ confirming that a mono-exponential fit is effectively not adequate for a correct description of the curves. When concentration increases, the difference between τ_1

and τ_2 also increases. This increased deviation from a mono-exponential behaviour indicates that fluctuations in concentration should increase with dye concentration. On the contrary, the sample with the lowest concentration (characterized by an inter-dye distance of 10.1 nm and a α_1 / α_2-ratio of $70/30$) possesses a mono-exponential behaviour more pronounced. This indicates that at low concentration, fluctuations are not sufficient to modify the local lifetime. This interpretation is confirmed by the corresponding value of $\bar{\tau}$=3.35 ns that is not too far from that of isolated fluorescein (4.0±0.2 ns).

Second reason for which a single population can be described by a multi-exponential law.
Second, in presence of energy transfer towards quenchers, this rapid quenching transforms the intensity evolution in a non-exponential decay obeying to an equation derived from the Forster theory (7):

$$I(t) = I_0 \exp(-t/\tau - 2\gamma\left(\frac{t}{\tau}\right)^{1/2}) \qquad (7)$$

in which τ is the lifetime, γ a coefficient dependent on the quencher concentration and 1/2 is a coefficient that depends on the dimensionality of the problem (1/6, 1/3 or 1/2 in spaces of dimension 1,2 and 3 respectively).

Table II. Lifetime decay fit of experimental data using a two-term exponential functions and the modified equation $I(t) = I_0 \exp(-t/\tau - 2\gamma\left(\frac{t}{\tau}\right)^{1/2})$. Of great interest are the values τ and γ that are now used in the paper to evaluate the radiative and non-radiative rates.

gold	<d_{FITC}>	α_1	τ_1 (ns)	α_2	τ_2 (ns)	χ	$\bar{\tau}$ (ns)	τ(ns)	γ
0	10,1	6900	3,776	3102	1,845	908	3,35	3,71	0,16
0	8,6	5467	3,785	4822	1,829	719	3,20	3,58	0,18
0	6,7	5450	3,339	4779	1,375	599	2,81	3,43	0,27
0	5	5192	2,830	4960	0,899	708	2,38	3,59	0,51
0	4	4612	2,656	5574	0,589	1133	2,22	4,18	0,95
5	11,5	3023	4,95	6977	2,885	872	3,63	3,65	0
5	9,5	1862	5,1019	8473	2,966	1180	3,55	3,57	0
5	7,6	1735	5,2014	8666	3,1042	1125	3,64	3,65	0
5	6,1	1976	5,2337	8288	3,1172	1061	3,72	3,73	0
5	4,5	2344	5,3447	7929	3,291	1053	3,96	4.02	0
5	3,5	7375	4,39	2365	1,6221	951	4,09	4,04	0
5	2,7	8473	3,992	1460	0,6292	1005	3,90	3.96	0

2. Synthesis of FITC doped silica nanoparticles (fluoSiOx)

The fluorescent dye solution was prepared by direct dissolution of the established FITC amount into the APTES under stirring at the room temperature, in a proportion at least $n_{APTES}/n_{FITC}=20$.

Quaternary W/O microemulsion was prepared by mixing 2.27 ml of Triton X-100 (surfactant), 2.31 ml of n-hexanol (co-surfactant), 9.61ml of cyclohexane (oil) and 0.61 ml of water at pH 5.5. After 5 min, 0.040 ml of the fluorescent dye solution was added to the microemulsion solution, followed by addition of 0.020 ml of APTES and 0.289 ml of TEOS. After 30 min, the silica polymerization reaction was completed by adding 0.173 ml of NH_4OH and then stirred for 24 h. Since the colloidal stability in water is required for their applications, a protective (and charged) shell was synthesized by adding 0.100 ml of TEOS and after 30 min, 0.050 ml of THPMP. The microemulsion was broken by the addition of ethanol to the microemulsion and followed by vortexing and centrifuging several times.

3. Synthesis of Au core - FITC doped silica shell nanoparticles (Au@fluoSiOx)

The fluorescent dye solution was prepared by direct dissolution of the established FITC amount into the APTES under stirring at the room temperature, in a proportion at least $n_{APTES}/n_{FITC}=20$.

Quaternary W/O microemulsion was prepared by mixing 2.10 ml of Triton X-100 (surfactant), 2.14 ml of n-hexanol (co-surfactant), 8.91 ml of cyclohexane (oil). The water phase consists of mixture of 0.595 ml of 16.7 mM $HAuCl_4 \cdot 3H_2O$, 0.595 ml of 32.8 mM MES and 0.198 ml of 412 mM $NaBH_4$ in order to synthesize the gold nanoparticle. After 5 min, 0.040 ml of the fluorescent dye solution was added to the microemulsion solution, followed by addition of 0.020 ml of APTES and 0.289 ml of TEOS. After 30 min, the silica polymerization reaction was completed by adding 0.173 ml of NH_4OH and then stirring for 24 h. Since the colloidal stability, a protective (and charged) shell was synthesized by adding 0.100 ml of TEOS and after 30 min, 0.050 ml of THPMP. The microemulsion was broken by the addition of ethanol to the microemulsion and followed by vortexing and centrifuging several times.

4. Some TEM images showing that all particles contain a gold core.

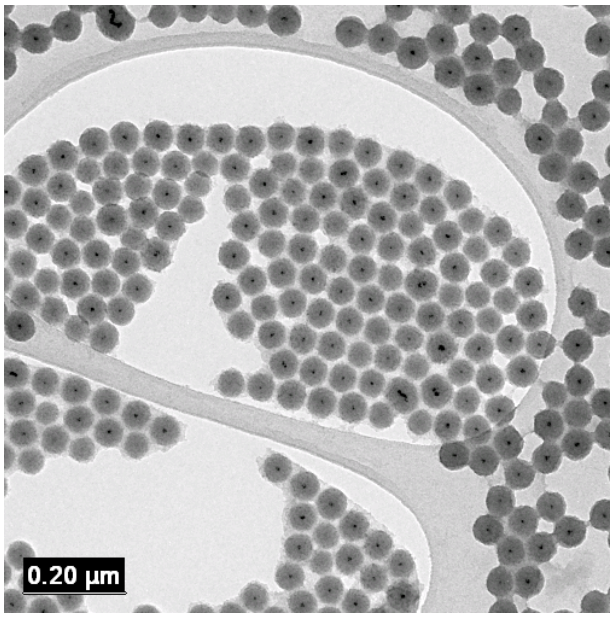

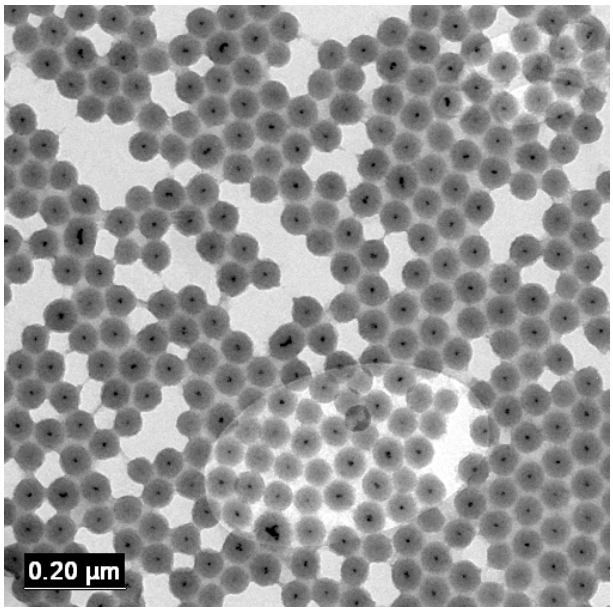

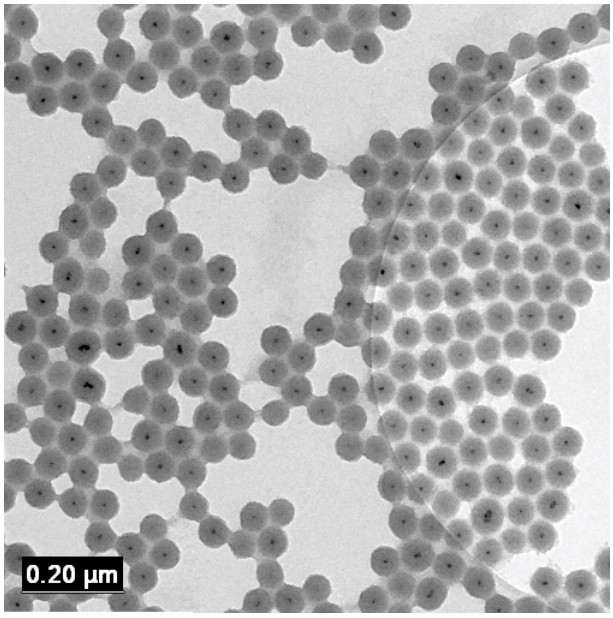

5. *Measurements of dye absorbance for determination of quantum yield.*

The extinction, $ext(\lambda)$, that is due to multiple mechanisms (dye absorption, gold absorption and particle scattering) is a linear combination of three terms : (i) the absorbance due to the presence of the dyes, $abs\_dye(\lambda)=n_{dye}\sigma_{dye}L$ with n_{dye} the concentration of dyes per volume unit, σ_{dye} their absorption cross section and L the optical length of the light within the solution, (ii) the absorbance due to the presence of gold particles, $abs\_gold(\lambda)=n_{particles}\sigma_{gold}L$ with $n_{particles}$ the concentration of gold cores (identical to that of particles) per volume unit and σ_{gold} the plasmon cross section and (iii) a quantity, $scat(\lambda)$, called scatterance and equal to $scat(\lambda)=n_{particles}\sigma_{scat}L$ with σ_{scat} the particles scattering cross section. This can be summarized in the following formulas:

$ext(\lambda)=abs\ (\lambda)+scat(\lambda)=abs\_dye(\lambda)+abs\_gold(\lambda)+scat(\lambda)$
or
$ext(\lambda)=n_{dye}\sigma_{dye}L+ n_{particles}\sigma_{gold}L+ n_{particles}\sigma_{scat}L$

The background that contains the scattering contribution of the sample to extinction is described by the Mie theory[i,ii,iii] and can be modelled according to different laws. The choice of the model depends on the parameter x that is the ratio of the characteristic dimension, d, of the scattering object and of the incoming wavelength λ: $x=\frac{2\pi d}{\lambda}$.[iv,v] If the particle size is very small compared to the light wavelength (x<<1), Rayleigh scattering occurs. In this case,

the scattering cross section is equal to $\sigma_{Ray} = \frac{2\pi^5}{3}\frac{d^6}{\lambda^4}\left(\frac{n^2-1}{n^2+2}\right)^2$ so that the background intensity varies as λ^{-4}. For larger sizes, when 0.1<x<10, the scattering intensity is given by the end of a Cauchy-Lorentz distribution,[vi] with a wavelength dependence approximated by a λ^{-2} law. In the core/shell studied here, we have two types of objects with different parameters x associated. Gold particles are characterized by a value of x ~0.1 and gold/polysiloxane particles by a value ~1. As the Rayleigh formula indicates that the cross section strongly increases with the size (power 6), the scattering generated by gold particles can be neglected in front of that induced by the whole particle. In this paper, we then chose the Lorentzian distribution for fitting all the backgrounds of the scattering samples. Figure 3 shows how the background can be removed for two solutions of gold/polysiloxane particles at the same concentration (0.04 µmol particles/L) containing (3a) or not (3c) 250 fluoresceins per particle. In both cases, the fit of the background with a Lorentzian distribution is excellent and leads after subtraction to the spectra of Figure 3b and 3d respectively. Extinction of Figure 3b contains both absorbance of gold plasmon (peaking at 536 nm) and fluorescein (493 nm) whereas that of Figure 3d contains only that of gold plasmon (536 nm). By assuming that the shape of the gold plasmon, *abs_gold*(λ), is the same in both samples, the two components of absorbance (Figure 3b) can be de-summed by subtracting from the spectrum of Figure 3b x times the spectrum of Figure 3d and refining x by a least square method. Figure 3e illustrates this operation of refinement by plotting the plasmon band for different values of x. We found that x=1.02 which confirms that the encapsulation of fluorophores does not modify the characteristic of the plasmon band (x was comprised from 0.99 to 1.02 for the other samples of the series). After all these extractions, we obtained finally (solid line of Figure 3f), the absorbance related to fluorescein, *abs_dye*(λ), the quantity that has to be used for determining the quantum yield. Very striking is that such an absorbance has exactly the same shape that fluorescein encapsulated in pure silica particles (dot line in Figure 3f) or that of fluorescein in water for low concentrations. This implies that the presence of gold do not perturb the repartition between monomers (the fluorescent species of fluorescein) and dimers (the fluorescein species acting as traps for light).

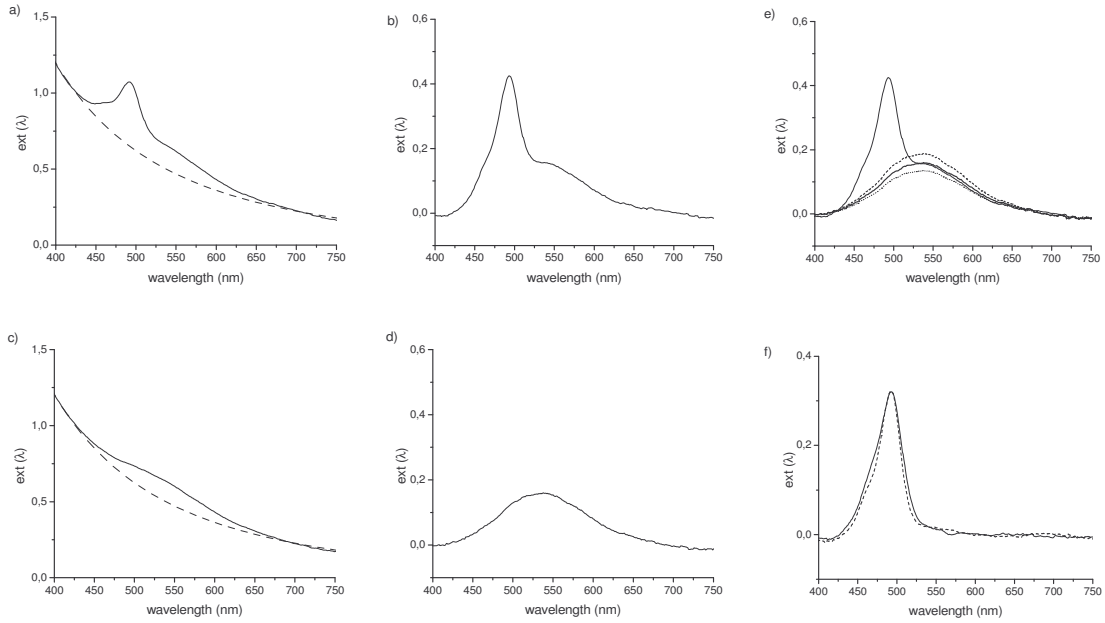

Figure 3. Schema for determining the absorbance due to fluorescein. Starting from the extinction spectra of a gold/polysiloxane particle (a) encapsulating or (d) not fluorescein, the background is removed (spectra (b) and (e) respectively). After de-summation of plasmon using a refining method (c), the absorbance is finally obtained (f – solid line). It has the same shape that in polysiloxane particles (f - dot line). Particle concentration is of 0.04 µmol particles/L (corresponding to an average distance between particles of 350 nm) and the fluorescein concentration is equal to 250 molecules/particle.

6. Overview of the historical interpretation of self-quenching problem in fluorescein solution

As other organic dyes, fluorescein molecules have well-know deficiencies [J. Lavorel, J. Phys. Chem., 1957, 61, 864] among which an important self-quenching of emission for high dye concentration. This effect has been know for about 100 years: in 1888 Walter noted that fluorescein emission increases with dilution and advanced the idea that fluorescein aggregation causes the quenching whereas the monomer forms irradiate in the green region of the visible spectrum. The dimerization of fluorescein molecules in protic solvent is probably due to hydrogen bonding [K. K. Rohatgi, A. K. Mukhopadhyay, J. Indian. Chem. Soc., 1972, 49, 1311] and is more pronounced in water than in organic solvents [O. Valdes-Aguilera, D. C. Neckers, Acc. Chem. Res., 1989, 22, 171]. The strength of the aggregation depends on the molecular structure of the dye, on the solvent, on the temperature and is influenced by the presence or the absence of electrolytes. The different structures of dimer aggregates have a large impact in the absorption spectrum. The dimerization process splits the excited-state of

the monomer form into two levels. For parallel dimers (H-type), the transition towards the lower energy excited state is forbidden and a blue shifted band appears in the absorption spectrum. On the contrary, for head-to-tail dimers (J-type), the transition to the higher energy excited state is forbidden and the spectrum shows a single band red-shifted. For dimers with intermediate geometries, both transitions are partially allowed and band splitting is observed[O. Kuhn, T. Renger, V. May, Chem. Phys., 1996, 204, 99]. According to the early results described in literature, [I. L. Arbeloa, Dyes Pigm., 1983, 4, 213 ; I. L. Arbeloa, J. Chem. Soc., Faraday Trans. 2, 1981, 77, 1725 ; I. L. Arbeloa, J. Chem. Soc., Faraday Trans. 2, 1981, 77, 1735] an increase in the fluorescein concentration modifies the absorption spectrum with the apparition of a second large band centred at 469 nm, closed to the monomer one (maximum at 493 nm) as reported in figure 4. Whereas the two fluorescein forms (monomers and dimers) display absorption bands, the dimer aggregates relax towards the ground state by vibronic transitions without radiative emission. Subsequently, it is clear that a sample containing dimer forms of dyes displays a smaller quantum yield value because a fraction of absorbed photons is not re-emitted. A wide discussion about the origin of self-quenching process started by Perrin [F. Perrin, Compt. Rend., 1924, 178, 1978] in 1924 and later by Forster [T. Forster, E. Konig, Z. Elektrochem., 1957, 61, 344] in 1951. They demonstrated that the presence of dimer forms of dyes in a solution was not merely sufficient to the self-quenching of fluorescence but needed other mechanisms to support. Indeed, the lifetime decay measurements displayed a progressive reduction of lifetime constant for higher concentrations, contrarily to the fact that dimer forms did not contribute in lifetime decays because they are non-fluorescent. Two hypotheses about the decrease in lifetime constant were formulated: the first one considers the possibility to excite dimer forms by collision between monomer and dimer fluorescein due to Brownian movement within solution. The slower lifetime of fluoresceins into such solution depends from an additive term $k_q[Q]$ proportional to the quencher concentration [Q] and was described in the Stern-Volmer equation.

$$\tau = \frac{1}{\Gamma_r + k_{nr} + k_q[Q]} \qquad (7)$$

The second hypothesis postulated a mechanism of energy transfer between fluorescein species, where the excitation jumps by dipole-dipole coupling through dyes also for larger distances. Forster indicated that the energy transfer process occurs whenever two entities, the donor and acceptor, are within the characteristic Forster distance R_0 and whenever suitable spectral overlap occurs. They pointed out that the transfer does not involve emission and re-

absorption of photons but only the energy exchange between coupled dipoles. The lifetime of donor molecule decreases because the presence of an additional pathway of relaxation as described in formula (8):

$$\tau = \frac{1}{\Gamma_r + k_{nr} + k_T} \qquad (8)$$

with the transfer rate k_T given by

$$k_T = \frac{1}{\tau_{DONOR}} \left(\frac{R_0}{r} \right)^6 . \qquad (9)$$

Based on depolarization measurements, Forster and Konig finally proposed that the self-quenching of fluorescence for fluorescein molecules was a combination of dimerization of monomers and the energy transfer of excitation towards the non-fluorescent species (dimers). The homotransfer between only monomer species does not decrease the measured lifetime. [J. N. Miller, Analyst, 2005, 130, 265 ; R. M. Clegg, Meth. Enzym., 1992, 211, 353] According to the Forster's theory, the fluorescein molecules entrapped within silica nanoparticles are subjected to the energy homotransfer because the small Stokes shift and the inter-dye distance comparable to the Forster's distance for fluorescein (estimated in 4.2 nm). The excitation may propagate within silica beads until the monomers emit or be lost into dimer traps.

6. Principles for determination of quantum yield.

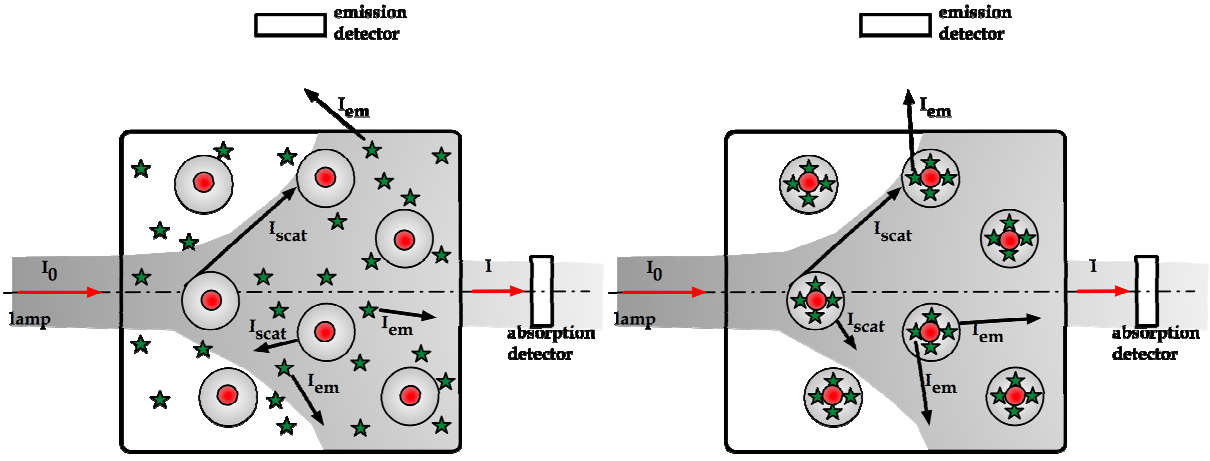

Schematic principle for measuring quantum yields using the method of William. Test sample (a) is compared to a reference sample (b) which has exactly the same scattering properties.

[i] Mie G., Ann. Der Phys., 1908, 25, 377
[ii] Roy A. K., Sharma S. K., J. Opt. A: Pure Appl. Opt., 2005, 7, 675
[iii] Fu Q., Sun W., Appl. Opt., 2001, 40, 1354
[iv] Bohren C. F., Huffman D., Absorption and scattering of light by small particles, 1983, John Wiley
[v] Ditchburn R. W., Light, 1963, Blackie & Sons
[vi] Lorenz L., Vidensk. Selk. Skr., 1890, 6, 1